

UNIVERSITY OF LONDON

IMPERIAL COLLEGE OF SCIENCE, TECHNOLOGY
AND MEDICINE

DEPARTMENT OF PHYSICS
APPLIED OPTICS GROUP

**Absolute length measurement using
multiple-wavelength phase-stepping
interferometry**

Andrew John Lewis MA

Thesis submitted for the degree of
Doctor of Philosophy of the University of London
and for the Diploma of Membership of Imperial College

November 1993

(2002 Re-print edition)

ABSTRACT

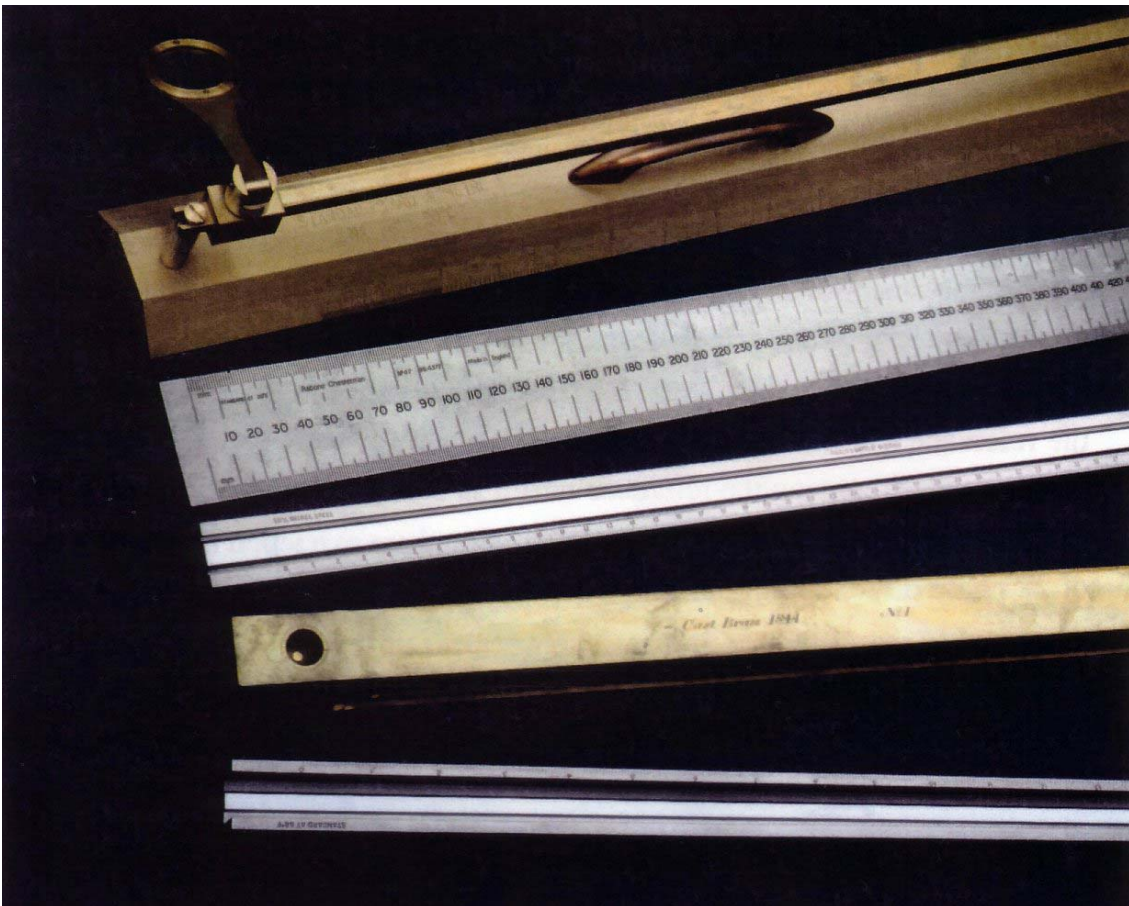
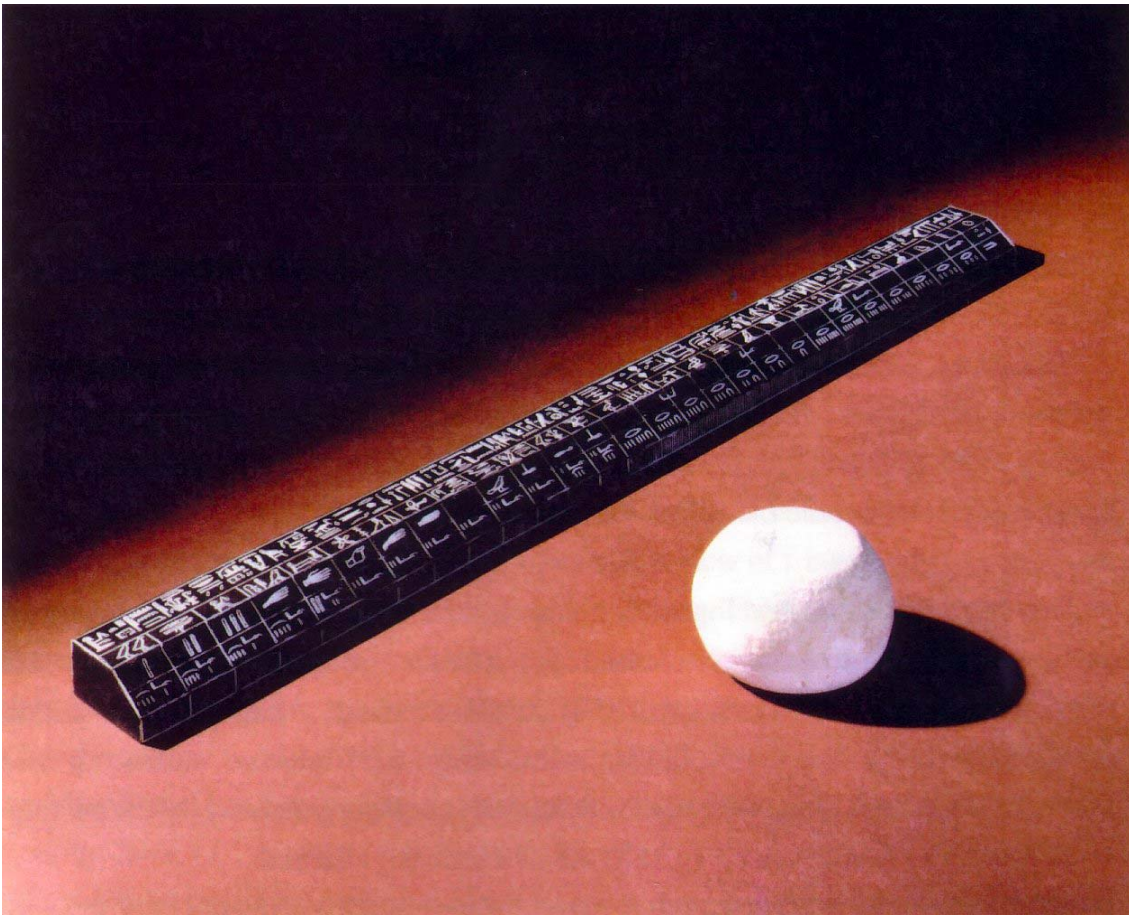
This thesis describes the design, construction, commissioning and testing of a new interferometer for the absolute measurement of length standards. The thesis starts with an introduction to the subject of length standards and length measurement by interferometry before considering various designs of interferometer. The design of the new interferometer is given in detail, including the operation of the lasers used as light sources. The alignment of the interferometer and the effects of incorrect alignment and collimation on the measured length are examined. A review of fringe analysis techniques is given, with an emphasis on phase-stepping algorithms. The 5-position algorithm used in the new interferometer is examined in more detail together with the phase-stepping actuator and its advantages over other devices. The data processing of images digitised in the interferometer is described, including the techniques developed for discontinuity removal and surface fitting. The measurement of the flatness and parallelism of the measuring faces of the length standards is described. The automated method of exact fractions is used to combine phase measurements at three wavelengths to allow accurate calculation of the length of the measured object, with a larger range than one or two-wavelength techniques. The techniques used for compensating for the refractive index of the air inside the interferometer chamber are summarised, with a comparison of calculated and directly-measured refractive index values, measured with a specially constructed refractometer. The thermal control of the interferometer is presented, including the use of the instrument to measure the thermal expansion coefficient of length standards, by measuring their lengths at different temperatures. Example results of length, flatness, parallelism, and thermal expansion are given for various sizes of length standard. A full uncertainty budget is calculated, allowing critical examination of the performance of the instrument. A chapter on conclusions is followed by several appendices.

PREFACE

This thesis describes the design, construction, commissioning and testing of a new multiple-wavelength phase-stepping interferometer for the measurement of length bars. This interferometer is called the NPL National Primary Length Bar Interferometer, or Primary Length Bar Interferometer (PLBI) for short. The instrument was designed and built at the National Physical Laboratory (NPL), Teddington. NPL was founded in 1900 and is the focus for the UK's National Measurement System.

The PLBI has been developed as a link between the realisation of the metre as a wavelength of a frequency-stabilised laser and the use of secondary length standards known as length bars, which are used as transfer standards to calibrate other standards or to verify the performance of instruments such as co-ordinate measuring machines (CMMs). The operation of the PLBI is described in a paper published by the author, which is reproduced in Appendix F (p 317). An overview is given here.

The PLBI is an interferometer of a modified Twyman-Green design, which measures the length of a bar in terms of the wavelength of the light emitted by calibrated frequency-stabilised lasers. The length, L , is calculated from the equation $L = (n + f)\lambda / 2$ where n is an integer (fringe order) and f is a fraction. In the interferometer, f is measured as a fringe fraction but n is initially unknown. The PLBI uses 3 wavelengths and measures a fringe fraction for each wavelength. The method of exact fractions is used to combine these 3 fractions with an estimate for L (within $\pm 9 \mu\text{m}$) to calculate L more accurately. In order to measure the fringe fractions with sufficient accuracy, Phase Stepping Interferometry is used to measure the fractions in terms of the phase difference between the reference and measurement beams. A 5-position phase-stepping algorithm is used which involves moving the reference mirror in 5 steps of size $\lambda/8$ for each wavelength and digitising the image at each step. Point-wise phase extraction is followed by removal of 2π phase discontinuities at fringe boundaries. After tilt removal, fringe fractions are measured as the difference in phase between pixels at the centre of the bar and those corresponding to the platen surface, in the 3 phase maps.



Egyptian Cubit (& mass standard) and more modern line standards of length

To my parents ...

CONTENTS

ABSTRACT	2
PREFACE	3
CONTENTS.....	7
LIST OF FIGURES.....	11
LIST OF TABLES.....	14
CHAPTER 1 INTRODUCTION.....	15
1.1 BACKGROUND.....	15
1.2 THE MEASUREMENT OF LENGTH	16
1.2.1 What is length?.....	16
1.2.2 The International System of units (SI).....	16
1.2.3 The definitions of the SI units	17
1.3 HISTORICAL UNITS OF LENGTH	19
1.3.1 Timetable of events	19
1.3.2 The first definition of the metre.....	20
1.3.3 The 1927 definition of the metre.....	21
1.3.4 The 1960 definition of the metre.....	22
1.3.5 The present (1983) definition of the metre	24
1.3.6 Limitations of the present realisation of the metre	26
1.3.7 Future realisations of the metre.....	27
1.4 SECONDARY LENGTH STANDARDS.....	29
1.4.1 Modern secondary length standards.....	29
1.4.2 Gauge blocks and length bars.....	29
1.4.3 Gauge blocks.....	30
1.4.4 Length Bars	31
1.4.5 Definitions and specifications for Reference Grade length bars.....	32
1.4.6 Calibration of End Standards of length	33
1.4.7 The rationale behind the development of the new interferometer	34
1.4.8 Traceability of length bar length measurements	35
1.5 CONTENTS OF THE THESIS	38
CHAPTER 2 REVIEW OF LENGTH MEASURING INTERFEROMETERS.....	41
2.1 THEORY OF INTERFEROMETRIC LENGTH MEASUREMENT.....	41
2.2 BASIC INTERFEROMETER TYPES	42
2.3 REVIEW OF SMALL FIELD, DYNAMIC INTERFEROMETERS	42
2.3.1 Fringe counting interferometry	42
2.3.2 Heterodyne fringe counting interferometry.....	45
2.3.3 Two-wavelength fringe counting interferometry	46
2.3.4 Other fringe counting systems.....	46
2.3.5 The effect of laser beam diffraction on measured length.....	47
2.4 REVIEW OF LARGE-FIELD INTERFEROMETER DESIGNS.....	48
2.4.1 The Fizeau interferometer.....	48
2.4.2 The Fabry-Perot interferometer.....	50
2.4.3 The Michelson interferometer.....	50
2.4.4 The Twyman-Green interferometer	51
2.4.5 Other designs of length measuring interferometer.....	52
2.5 PRIMARY LENGTH BAR INTERFEROMETER - BASIC INTERFEROMETER TYPE	53
2.5.1 The technique of 'wringing'.....	54
CHAPTER 3 THE DESIGN OF THE INTERFEROMETER.....	57
3.1 OPTICAL DESIGN OF THE INTERFEROMETER	57
3.1.1 Description of the interferometer	57
3.1.2 The interferometer chamber.....	61
3.2 DETAILS OF INTERFEROMETER COMPONENTS.....	64
3.2.1 Design of lasers used with the interferometer.....	64
3.2.1.1 Helium-neon laser theory	64
3.2.1.2 Single mode laser wavelength stabilisation schemes	67
3.2.1.3 Laser frequency-stabilisation using saturated absorption	68
3.2.1.4 Zeeman-Stabilised 633 nm Lasers.....	69

3.2.1.5 Calibration of the Zeeman-stabilised 633 nm laser	72
3.2.1.6 Calibration of 612 nm and 543 nm lasers	73
3.2.2 The optical fibre illumination delivery system	73
3.2.3 Reference mirror assembly	76
3.2.4 Design of the imaging optics	78
3.2.5 Design of length bar supports	80
3.2.6 Length bar support carriage design	82
3.2.7 Design of the adjustable mirror in the measurement arm	85
3.2.8 External equipment rack and computing equipment	85
3.3 DOUBLE-ENDED INTERFEROMETRY	88
3.3.1 The wringing film thickness	88
3.3.2 Surface roughness	88
3.3.3 Phase change on reflection	89
3.3.4 Effect of surface form errors of measuring faces	91
3.4 OTHER DOUBLE-ENDED DESIGNS	91
3.5 DOUBLE-ENDED INTERFEROMETRY IN THE PRIMARY LENGTH BAR INTERFEROMETER	93
3.5.1 Analysis of new double-ended interferometer	95
3.5.2 Double-ended phase-stepping	96
CHAPTER 4 ALIGNMENT, COHERENCE AND OPTICAL TESTING	99
4.1 ALIGNMENT OF THE INTERFEROMETER	99
4.1.1 Approximate alignment of interferometer	99
4.1.1.1 Laser beam launching into fibres	99
4.1.1.2 Component positioning in interferometer	100
4.1.1.3 Fibre positioning in collimator	100
4.1.1.4 Reference mirror alignment	100
4.1.1.5 Measurement beam alignment	101
4.1.1.6 Alignment of length bars with measurement beam	101
4.1.1.7 Alignment for double-ended interferometry	102
4.1.2 Accurate alignment of the interferometer	103
4.1.2.1 Cosine error due to measurement beam mis-alignment	104
4.1.2.2 Alignment of the three interferometer axes	105
4.1.2.3 Two-fibre autocollimation technique	105
4.1.3 Obliquity effect due to position and size of light source	108
4.1.3.1 Obliquity effect due to source size - full derivation	109
4.1.4 Collimation check using a shearing plate interferometer	111
4.1.5 Tilt in the measurement beam	112
4.1.5.1 Prismatic dispersion at the beamsplitter	114
4.1.5.2 Methods for compensation of tilt	114
4.1.6 Chromatic aberration - tolerance on collimator focal position	115
4.1.7 Optical component quality and spherical aberration	116
4.1.7.1 Quality of optical components	116
4.1.7.2 Effect of spherical aberration in collimator	116
4.1.8 Effect of squareness of length bar on measured length	118
4.2 COHERENCE IN THE INTERFEROMETER	119
4.2.1 Temporal coherence	120
4.2.2 Spatial coherence	121
4.2.2.1 An approximate estimate of the spatial coherence	121
4.2.2.2 Detailed estimate of the spatial coherence	122
CHAPTER 5 FRINGE ANALYSIS & PHASE-STEPPING INTERFEROMETRY	135
5.1 ANALYSIS OF INTERFERENCE FRINGES	135
5.1.1 Introduction to interference fringe analysis	135
5.1.2 Fringe skeletonisation methods	137
5.1.3 Fourier transform methods	137
5.1.4 Temporal heterodyning methods	138
5.1.5 Spatial heterodyning methods	138
5.1.6 Phase locking methods	139
5.1.7 Summary of phase measurement methods	139
5.2 PHASE-STEPPING INTERFEROMETRY (PSI)	140
5.2.1 History of PSI	140
5.2.2 Basic theory of PSI	141
5.2.3 Derivation of generic PSI equations	141
5.2.4 Typical applications of PSI	144

5.2.5 Phase variation methods for PSI	144
5.3 PHASE STEPPING TECHNIQUES	144
5.3.1 Basic phase-stepping techniques	144
5.3.2 Phase-shifting interferometry	147
5.3.3 Four quadrant arctangent routine	147
5.3.4 Two position phase-stepping technique	148
5.3.5 Three position phase-stepping technique	149
5.3.6 Four position phase-stepping technique	150
5.3.7 Errors for three and four position techniques	150
5.3.7.1 Error due to phase stepper error	150
5.3.7.2 Error due to detector response	153
5.3.7.3 Error due to multiply-reflected beams	154
5.3.7.4 Error due to quantisation noise during digitisation	155
5.4 AN ERROR-COMPENSATING FIVE POSITION TECHNIQUE	156
5.5 IMPLEMENTATION OF THE FIVE POSITION TECHNIQUE IN THE PRIMARY INTERFEROMETER	160
CHAPTER 6 DATA PROCESSING	165
6.1 OVERVIEW OF THE DATA PROCESSING	165
6.2 COMPUTING SYSTEM	167
6.3 IMAGE PROCESSING	168
6.3.1 Interferogram digitisation	168
6.3.2 Phase extraction	170
6.3.3 Discontinuity removal	171
6.4 MULTIPLE-WAVELENGTH INTERFEROMETRY	175
6.4.1 Multiple wavelength analysis	175
6.4.2 Limit to multiple-wavelength technique due to source instability	179
6.4.3 Multiple wavelength algorithm - method of exact fractions	180
6.5 FLATNESS AND PARALLELISM MEASUREMENTS	184
6.5.1 Measurement of parallelism (variation)	184
6.5.2 Measurement of flatness	186
6.5.3 Example measurements	187
6.6 COMPUTER PROGRAM	189
6.7 DOUBLE-ENDED ANALYSIS	192
CHAPTER 7 REFRACTOMETRY	197
7.1 REFRACTIVITY OF AIR	197
7.1.1 Dispersion factor	197
7.1.2 Density factor	198
7.2 EDLÉN'S EQUATIONS FOR THE REFRACTIVITY OF AIR	199
7.2.1 Refractivity of standard air	199
7.2.2 Corrections for temperature, pressure, water vapour and CO ₂	199
7.3 EFFECTS OF PRESSURE, TEMPERATURE, HUMIDITY AND CO ₂ ON REFRACTIVITY	201
7.3.1 Pressure measurement	201
7.3.2 Temperature measurement	202
7.3.3 Humidity measurement	203
7.3.4 Carbon dioxide measurement	204
7.3.5 Air parameter measurement order	204
7.4 OTHER WAVELENGTH COMPENSATION TECHNIQUES	205
7.4.1 Two-wavelength compensation	205
7.4.2 Gas refractometry	205
7.4.2.1 Gas refractometer design	206
7.4.2.2 Refractometer operation	207
7.4.2.3 Corrections and errors	207
7.4.2.4 Comparison between Edlén and refractometer	209
7.5 ADDENDUM	212
CHAPTER 8 THERMAL EXPANSION	215
8.1 THERMAL REQUIREMENTS	215
8.2 TEMPERATURE CONTROL SYSTEM	217
8.3 TEMPERATURE MEASUREMENT SYSTEM	219
8.3.1 PRTs and resistance bridge details	219
8.3.2 Calibration of PRTs	220
8.3.3 Temperature measurements using ITS-90	221

8.4 STABILITY OF TEMPERATURES INSIDE CHAMBER.....	223
8.4.1 Measurements at 20 °C.....	223
8.4.2 Heating from 20 °C to 30 °C.....	224
8.5 CALCULATION OF THERMAL EXPANSION COEFFICIENTS	226
8.6 ERRORS IN α AND β	227
8.6.1 Error propagation method - calculation of error in α and β	227
8.6.2 Least-squares fit to data with errors in both coordinates	230
8.7 EXAMPLE OF THERMAL EXPANSION MEASUREMENT	231
CHAPTER 9 PERFORMANCE OF THE INTERFEROMETER	235
9.1 ASSESSMENT OF THE INTERFEROMETER	235
9.2 FRINGE FRACTION MEASUREMENTS	236
9.3 ZERO-LENGTH MEASUREMENTS	237
9.4 CENTRAL LENGTH MEASUREMENTS.....	238
9.5 FLATNESS & PARALLELISM MEASUREMENTS	240
9.6 THERMAL EXPANSION MEASUREMENTS.....	242
9.7 GAUGE BLOCK MEASUREMENTS.....	245
9.8 DOUBLE-ENDED MEASUREMENTS	245
9.9 CONCLUSIONS ON PERFORMANCE.....	247
CHAPTER 10 UNCERTAINTY OF MEASUREMENTS	249
10.1 THE NATURE OF ERRORS	249
10.1.1 The 'orthodox' theory of errors	249
10.1.2 Combination of errors	250
10.1.3 Random errors.....	251
10.1.4 Systematic errors.....	252
10.2 BIPM RECOMMENDATIONS ON ERROR ASSESSMENT	252
10.3 COMPARISON OF 3 THEORIES OF ERROR AND RECOMMENDATIONS.....	253
10.4 SOURCES OF UNCERTAINTY	256
10.4.1 Air pressure measurement	257
10.4.2 Air temperature measurement.....	258
10.4.3 Air humidity measurement.....	259
10.4.4 Air CO ₂ measurement & Edlén's equations.....	260
10.4.5 Laser wavelength.....	261
10.4.6 Mechanical - optical effects	262
10.4.7 Bar expansivity at 20 °C	263
10.5 SUMMATION OF UNCERTAINTIES	264
10.6 POSSIBLE STEPS TO IMPROVE THE ACCURACY.....	266
10.7 COMBINED UNCERTAINTY BUDGETS OF INSTRUMENTS.....	266
CHAPTER 11 CONCLUSIONS	269
11.1 CONCLUSIONS	269
11.2 PROPOSALS FOR IMPROVEMENTS	271
11.3 ACKNOWLEDGEMENTS.....	274
APPENDIX A OPTO-MECHANICAL EQUIPMENT LIST.....	277
APPENDIX B QUALITY OF OPTICAL SURFACES	281
APPENDIX C FLEXING OF LENGTH BARS.....	283
C.1 FLEXING OF A LENGTH BAR DUE TO ITS OWN WEIGHT	283
C.2 DERIVATION OF POSITIONS OF AIRY POINTS	284
C.3 COMPENSATION FOR MASS OF WRUNG FLAT	287
C.4 EFFECT OF FLEXURE OF BARS ON THEIR LENGTH	293
APPENDIX D PRISMATIC COMPRESSION OF LENGTH BARS	295
APPENDIX E CONNECTORS & CONNECTIONS	299
APPENDIX F PUBLICATIONS BY THE AUTHOR	305
END NOTE	323

LIST OF FIGURES

Figure 1.1 - Cross-section of International Prototype Metre designed by Tresca	21
Figure 1.2 - Frequency chain for methane laser frequency determination	24
Figure 1.3 - Trends in accuracy of determination of length and speed of light	28
Figure 1.4 - A set of gauge blocks, 2 long series gauge blocks and 2 length bars	30
Figure 1.5 - Gauge blocks being wrung to a platen.....	31
Figure 1.6 - NPL Length Bar Machine	34
Figure 1.7 - Traceability of length measurements	35
Figure 1.8 - Iodine-stabilised He-Ne Primary laser	36
Figure 1.9 - NPL design Zeeman stabilised laser	37
Figure 2.1 - Schematic diagram of a fringe counting interferometer	43
Figure 2.2 - Use of fringe counting to measure the length of an object.....	44
Figure 2.3 - Schematic diagram of a heterodyne fringe counter.....	45
Figure 2.4 - Laser beam waist - alteration of effective propagation speed.....	47
Figure 2.5 - Standard Fizeau interferometer.....	49
Figure 2.6 - Modification to Fizeau interferometer	49
Figure 2.7 - Normalised intensity profiles of fringes in a Fizeau interferometer.....	50
Figure 2.8 - Fabry-Perot interferometer	50
Figure 2.9 - Michelson interferometer.....	51
Figure 2.10 - Twyman-Green interferometer	51
Figure 2.11 - Coherence depth doubling by positioning of reference mirror	52
Figure 2.12 - Kösters-Zeiss interference comparator	53
Figure 2.13 - Twyman-Green interferometer for the measurement of length bars	53
Figure 2.14 - Wringing a platen onto the end of a length bar	54
Figure 3.1 - Schematic design of interferometer optics.....	58
Figure 3.2 - Diagram showing the opto-mechanical components of the interferometer	59
Figure 3.3 - Perspective view of optical components and directions of beams	60
Figure 3.4 - Lid of chamber	63
Figure 3.5 - Aluminium 'collar' used as side walls of chamber.....	63
Figure 3.6 - Optical table used as base of interferometer chamber	64
Figure 3.7 - Energy levels in the He-Ne gas laser for 632.8 nm radiation	65
Figure 3.8 - Schematic diagram of an iodine-stabilised He-Ne laser.....	69
Figure 3.9 - Magnetic splitting of neon	70
Figure 3.10 - Refractivities of two Zeeman modes in 632.8 nm laser mode	70
Figure 3.11 - Calibration scheme for Zeeman stabilised laser	72
Figure 3.12 - Synchronisation diagram for red Zeeman stabilised laser	73
Figure 3.13 - Focusing of laser beam into fibre core	74
Figure 3.14 - Coupling efficiency of fibre launch.....	74
Figure 3.15 - Three source coupling using 2:2 couplers	75
Figure 3.16 - Three source coupling and return spot detection using 2:1 couplers	75
Figure 3.17 - Reference mirror assembly	77
Figure 3.18 - Exaggerated tilting of reference mirror when translating horizontally.....	78
Figure 3.19 - The imaging optics of the NPLBI	79
Figure 3.20 - Comparison of end face sizes of length bars & long series gauge blocks	79
Figure 3.21 - Video prints showing different diffraction effects at the edge of bars	80
Figure 3.22 - Length bar supports with integral PRTs, end view	81
Figure 3.23 - Length bar supports with integral PRTs, side view.....	81
Figure 3.24 - Length bar support carriage.....	83

Figure 3.25 - View of carriage, supports, length bars and optics inside chamber.....	84
Figure 3.26 - Flexure system for tilting mirror.....	85
Figure 3.27 - Schematic front view of equipment rack.....	86
Figure 3.28 - Schematic diagram of interferometer & external equipment	87
Figure 3.29 - Double-ended interferometer of Dorenwendt.....	91
Figure 3.30 - Analysis of triangular interferometer of Dorenwendt	92
Figure 3.31 - Additional roof-mirror optics for double-ended interferometry.....	94
Figure 3.32 - Double ended image	95
Figure 3.33 - Analysis of new double-ended interferometry.....	95
Figure 4.1 - Aligning the measurement beam with the length bar	101
Figure 4.2 - Incorrect adjustment of roof mirror orthogonality	103
Figure 4.3 - Correct adjustment of roof mirror orthogonality.....	103
Figure 4.4 - Cosine error of measurement beam	104
Figure 4.5 - Three fibre system	105
Figure 4.6 - Autocollimation arrangement	106
Figure 4.7 - Detected intensity during (a) radial and (b) axial positioning of the fibre	107
Figure 4.8 - Obliquity effect due to a circular aperture on axis of interferometer	109
Figure 4.9 - Convergence of un-collimated wavefront	112
Figure 4.10 - Difference in tilt between wavelengths 633 nm, 612 nm, 543 nm	113
Figure 4.11 - Chromatic dispersion - effect on focal length of collimator.....	115
Figure 4.12 - Spherically aberrated wavefront	116
Figure 4.13 - Interference between two spherically aberrated beams.....	117
Figure 4.14 - Non-square, singularly non-parallel length bar	118
Figure 4.15 - Coherence of an extended source with slit and screen	122
Figure 4.16 - Source sphere centred on image plane origin.....	123
Figure 4.17 - Coherence between source and image planes separated by R.....	125
Figure 4.18 - Coherence from a uniform circular source centred at origin.....	126
Figure 4.19 - Variation of coherence for the Primary Length Bar Interferometer.....	129
Figure 4.20 - Section through figure 4.19 showing detail	129
Figure 4.21 - Region of figure 4.19 about coherence limit of 0.88.....	130
Figure 4.22 - Double-ended interferogram showing different fringe contrasts.....	131
Figure 4.23 - Double-ended images for three wavelengths	132
Figure 5.1 - Example Twyman-Green interferometer for optical testing	136
Figure 5.2 - Idealised interferometer for testing surfaces.....	142
Figure 5.3 - Errors in general 3, 4 and 5-position techniques for phase step error.....	152
Figure 5.4 - Variation of phase step factor as a is varied.....	157
Figure 6.1 - Flow diagram of data processing.....	166
Figure 6.2 - Organisation of framestore memory	168
Figure 6.3 - Simulated intensity arrays for the first 4 digitised images	169
Figure 6.4 - Typical digitisation histogram	170
Figure 6.5 - Typical digitisation histogram but with more dark fringes in the image	170
Figure 6.6 - Simulated phase map	171
Figure 6.7(a) - Discontinuity removal 1st pass across top line of image	172
Figure 6.7(b) - Discontinuity removal - comparison of phase of top line with next	172
Figure 6.7(c) - Discontinuity removal 1st pass - continuation until middle of image	173
Figure 6.8 - Discontinuity removal 2nd pass from left to right.....	173
Figure 6.9 - Simulated phase map after discontinuity removal	174
Figure 6.10 - Phase maps after discontinuity and tilt removal,	175
Figure 6.11 - Coincidences for two wavelengths 633 nm & 543 nm	177
Figure 6.12 - Coincidences for three wavelengths 633 nm, 543 nm, 612 nm.....	178
Figure 6.13 - Measurement of deviation from parallelism of measurement faces	185

Figure 6.14 - Measurement of deviation from flatness of measurement face	186
Figure 6.15 - Example showing errors in the phase map	187
Figure 6.16 - Example measurements of flatness and parallelism (variation).....	188
Figure 6.17 - Program flowchart (simplified).....	189
Figure 6.18 - Example printout from interferometer	192
Figure 7.1 - Dispersion of standard air over the region 350 nm - 700 nm.....	198
Figure 7.2 - Gas refractometer schematic	206
Figure 7.3 - Comparison of Edlén and refractometer	210
Figure 7.4 - Comparison of Edlén and refractometer	210
Figure 7.5 - Periodic error due to drift	211
Figure 8.1 - Spiral of pipework on lid and baseplate.....	217
Figure 8.2 - Heating, cooling and insulation of interferometer	218
Figure 8.3 - Fringe distortion due to opening of chamber at raised temperature	219
Figure 8.4 - Triple point of water cell used for temperature calibrations.....	221
Figure 8.5 - Stability of air temperature inside chamber at 20 °C	223
Figure 8.6 - Stability of bar and air temperatures at 20 °C.....	224
Figure 8.7 - Comparison of heating rates using PRT on baseplate or in water bath	225
Figure 8.8 - Temperature measurements of air temperature gradients	226
Figure 8.9 - Least squares quadratic fit to thermal expansion data for 1000 mm bar	232
Figure 9.1 - Comparison of length bar measurements from three instruments.....	239
Figure 9.2 - Photograph of screen showing results for a 1000 mm length bar	241
Figure 9.3 - Example measurement of a gauge block	245
Figure 9.4 - Double-ended image, stored in framestore during measurement.....	246
Figure 9.5 - Three phase maps obtained during a double-ended measurement.....	246
Figure 10.1 - Four classes of experimental error.....	254
Figure 10.2 - Plot of total uncertainty in length measurement over range 0.1 - 1.5 m	265
Figure C.1 - Bar supported at two points	284
Figure C.2 - Effect of support point position, a , on change in length, dL , of bar.....	286
Figure C.3 - Bar supported at new support points with flat attached to one face	287
Figure C.4 - Variation in vertical position and gradient (dashed line) of neutral plane.....	294
Figure D.1 - Compression on cross section of bar	295
Figure D.2 - Contraction of a steel length bar, standing vertically	298
Figure E.1 - Electronics rack, left side view of connectors	299
Figure E.2 - Electronics rack, right side view of connectors.....	300
Figure E.3 - Pump control using solid state relay	300
Figure E.4 - Motor power connections from motor to PSU	301
Figure E.5 - Motor direction control, from joystick microswitches to PSU board	301
Figure E.6 - Motor inhibit connections, microswitches on stage to PSU board	302
Figure E.7 - Motor control from joystick switches to motor.....	302
Figure E.8 - Low voltage PZT power supply connections.....	303
Figure E.9 - High voltage PZT power supply connections	303
Figure E.10 - Gas sample flow connections.....	304

LIST OF TABLES

Table 1.1 - The 7 base units of the SI system	17
Table 1.2 - Realisations of the SI units at NPL	18
Table 1.3 - Recommended wavelengths for realisation of the metre	26
Table 1.4 - Tolerances: parallelism, flatness & length for reference bars to BS 5317	33
Table 2.1 - Typical fringe interpolation errors (FT Technologies FT612AS)	44
Table 5.1 - Summary of phase measurement techniques	140
Table 5.2 - Four-quadrant lookup table	148
Table 5.3 - Non-linearity effects present for R-step algorithm	153
Table 5.4 - Phase measurement error (radians) due to digitisation quantisation noise.....	156
Table 7.1 - Typical variations in air temperature, pressure, humidity and CO ₂	201
Table 7.2 - Effect of air temperature, pressure, humidity & CO ₂ content on refractivity.....	201
Table 7.3 - Errors in pressure reading due to change from 0% to 70%RH.....	202
Table 8.1 - Constants used in ITS-90 reference equation	222
Table 8.2 - Calibration data for interferometer PRTs.....	222
Table 8.3 - Error in measured value of α (10^{-6} K^{-1}).....	230
Table 8.4 - Measured thermal expansion data for a 1000 mm length bar.....	231
Table 9.1 - Fringe fraction sample results	237
Table 9.2 - Results of zero-length measurements	237
Table 9.3 - Comparison results of length bars measured in three instruments	238
